Polymer 50 (2009) 467–474

Contents lists available at ScienceDirect

Polymer

journal homepage: www.elsevier.com/locate/polymer

Synthesis and association properties of thermoresponsive and permanently cationic charged block copolymers

Maria Loreta Patrizi [a], Marco Diociaiuti [c], Donatella Capitani [b], Giancarlo Masci [a,*]

[a] Department of Chemistry, University of Rome La Sapienza, Piazzale Aldo Moro 5, 00185 Rome, Italy
[b] Institute of Chemical Methodologies, CNR, Via Salaria km 29300, 00016 Monterotondo Stazione, Rome, Italy
[c] Dipartimento di Tecnologie e Salute, Istituto Superiore di Sanita, Viale Regina Elena 299, 00161 Roma, Italy

ARTICLE INFO

Article history:
Received 25 September 2008
Received in revised form
13 November 2008
Accepted 17 November 2008
Available online 25 November 2008

Keywords:
Atom transfer radical polymerization
Micellization
Thermosensitive

ABSTRACT

Atom transfer radical polymerization (ATRP) was used to prepare thermosensitive cationic block copolymers of (3-acrylamidopropyl)-trimethylammonium chloride (AMPTMA) and *N*-isopropylacrylamide (NIPAAM) with different block lengths. By using ethyl-2-chloropropionate (ECP) as initiator and CuCl/$CuCl_2$/tris(2-dimethylaminoethyl)amine (Me_6TREN) catalytic system in DMF:water 50:50 (v/v) mixtures at 20 °C the polymerization was controlled. The association properties in NaCl aqueous solution were studied as a function of temperature and polymer concentration by dynamic light scattering, NMR spectroscopy, fluorescence spectroscopy and energy filtered-transmission electron microscopy. The block copolymers formed micellar aggregates above the lower critical solution temperature (LCST) of pNIPAAM. The LCST is strongly influenced by the relative length of the two blocks and is significantly higher than that of pure pNIPAAM. The size of core and shell of the micelles is discussed in terms of block copolymer composition.

1. Introduction

In recent years, polymers that can self-assemble in aqueous solution have received more and more attention due to their ability to form nanostructured associated species like micelles or vesicles with a hydrophobic core and a hydrophilic shell [1–4]. One of the most interesting polymeric architectures that are able to give rise to this phenomenon is double hydrophilic block copolymers. This is a special kind of architecture having both the blocks soluble in water in given conditions. By a proper stimulus such as temperature, pH, or ionic strengths, one of the blocks can become insoluble in water and the block copolymer self-assemble by forming micelles or vesicles with the "sensitive" block in the hydrophobic core. Among the available stimulus responsive polymers, thermally responsive materials are advantageous for biological applications because of the stringent pH requirements in mammalian. One of the most interesting "sensitive" polymer is poly(*N*-isopropylacrylamide) (pNIPAAM), a thermoresponsive polymer which is water soluble at room temperature and is able to give a coil-to-globule transition above 32 °C (the LCST, lower critical solution temperature) [5,6]. NIPAAM copolymers have attracted a lot of attention as the LCST in water is close to body temperature and may therefore be useful in the biomedical field as a stimulus-sensitive material. The synthesis of pNIPAAM block copolymers received a significant stimulus by the development of the so-called "living" radical polymerization (LRP). Several pNIPAAM block copolymers have been prepared by both reversible addition–fragmentation chain transfer (RAFT) [7–18] and atom transfer radical polymerization (ATRP) [19–29]. Nevertheless, to our knowledge the direct synthesis of pNIPAAM block copolymers with permanently charged quaternized cationic monomers has not been reported yet. Quaternized cationic homopolymers and copolymers are an important class of materials since they exhibit bactericidal and fungicidal activities [30,31] and can be used to develop self-disinfecting surfaces [32]. For instance, they can be used for a number of applications in hospital surfaces and medical devices, filtration devices, plastic applications, food manufacturing, marine applications. Furthermore, recently it has been demonstrated that diblock copolymer micelles comprising a pH sensitive block core and a quaternized cationic block corona can be used as nanosized templates for the deposition of silica from aqueous solutions [33].

Therefore, block copolymers consisting of a hydrophobic or stimuli sensitive block and quaternized cationic hydrophilic block could have very interesting potential applications. Here we report the first example of direct synthesis by ATRP of double hydrophilic block copolymers of NIPAAM with a quaternized acrylamide based monomer, (3-acrylamidopropyl)-trimethylammonium chloride (AMPTMA). Block copolymers with different compositions were

* Corresponding author. Tel.: +39 06 49913677.
E-mail address: giancarlo.masci@uniroma1.it (G. Masci).

0032-3861/$ – see front matter © 2008 Elsevier Ltd. All rights reserved.
doi:10.1016/j.polymer.2008.11.023

synthesized and their temperature induced association properties in aqueous solution were studied.

2. Experimental section

2.1. Materials

Tris(2-dimethylaminoethyl)amine (Me_6TREN) was synthesized as previously described [34]. CuCl from Fluka was washed with acetic acid followed by methanol to remove impurities. $CuCl_2$ from Fluka was used as-received. (3-acrylamidopropyl)-trimethylammonium chloride 75% in water (AMPTMA) from Aldrich was used as-received. *N*-isopropylacrylamide (NIPAAM, Aldrich) was recrystallized from hexane end dried under vacuum prior to use. Ethyl-2-chloropropionate (ECP, Aldrich) and all other reagents were used as-received.

2.2. Polymerization of AMPTMA

In a typical polymerization in DMF:water 50:50 (v/v), [AMPTMA]:[ECP]:[CuCl]:[Me_6TREN] = 60:1:1:1 and [AMPTMA] = 1.25 M, 6 mL of AMPTMA 75% w/v aqueous solution (21.8 mmol), 3.5 mL of water and 8.7 mL of DMF were introduced in a Schlenk tube and degassed by purging with argon. In a 25 mL, two-necked round-bottomed flask previously degassed by three vacuum–argon cycles, a Cu(I)–Me_6TREN water stock solution was prepared by adding 6 mL of degassed water to 72 mg (0..72 mmol) of CuCl and 180 μL (0.72 mmol) of Me_6TREN. After taking from the Schlenk tube an initial sample to measure the monomer concentration at $t = 0$, degassed ECP (46.2 μL, 0.36 mmol) and 3 mL of the freshly prepared Cu(I)–Me_6TREN water stock solution were added to the AMPTMA solution. The solution turned light green as the complex formation occurred. The polymerization was carried out at 20 °C. To measure the monomer conversion by HPLC, samples were withdrawn and diluted up in the eluent. At the same time, a given amount of reaction mixture was withdrawn and diluted in the GPC eluent for the molecular weight determination. Before analysis, the samples were filtered with a 0.45 μm syringe filter.

To obtain purified pAMPTMA macroinitiator, at the end of the polymerization the mixture was diluted, bubbled with air for 5 min to stop the polymerization and extensively dialyzed against distilled water. The solid product was obtained by lyophilisation.

2.3. Chain-extension experiments

The first pAMPTMA block was synthesized as described in the preceding section using [AMPTMA]:[ECP]:[CuCl]:[Me_6TREN] = 50:1:1:1:1. When the conversion was approximately 97%, a degassed solution of AMPTMA (5 mL, 18.2 mmol, [AMPTMA]:[ECP] = 200:1), 1.8 mL of water and 3.6 mL of DMF was added. The conversion of the second AMPTMA feed reached 78% in about 300 min. GPC analysis was performed as previously described.

2.4. Synthesis of block copolymers p(*AMPTMA*-b-*NIPAAM*)

Block copolymers were synthesized using a "one-pot" method. pAMPTMA macroinitiators were prepared with the same procedure reported previously. When the conversion of AMPTMA reached about 98%, a solution of NIPAAM in DMF:H_2O 50:50 (v/v) was added in order to obtain 2 M NIPAAM concentration in the polymerization mixture. When the conversion reached the value necessary to obtain the targeted X_n value, the polymerization was stopped by diluting and bubbling with air for 5 min. The solid polymer was obtained by extensive dialysis and lyophilisation.

2.5. Characterization

2.5.1. ^1H NMR

^{1}H NMR spectra were recorded at 293 and 333 K on a Bruker AVANCE AQS600 spectrometer operating at 600.13 MHz, respectively, and equipped with a Bruker z-gradient probehead. Chemical shifts in D_2O were reported in ppm with respect to a trace of 2,2-dimethyl-2-silapentane-5-sulfonate sodium salt (DSS) used as an internal standard.

2.5.2. HPLC

HPLC experiments for the determination of monomer conversion were performed using a LabFlow 4000 HPLC pumps (LabService Analytica, Bologna, Italy) equipped with a Knauer K-2501 UV detector and a C18 (Phenomenex Luna, 5 μm) Column. AMPTMA was analyzed by eluting with water/acetonitrile/acetic acid 90/5/5 (v/v/v). NIPAAM was determined by eluting with water/acetonitrile 70/30 (v/v). The injection volume was 10 μL. DMF was used as internal standard.

2.5.3. GPC

Molecular weight distributions were obtained using a GPC system equipped with a LabFlow 4000 HPLC pump, TSK-GEL α-3000 (30 cm × 7.8 mm ID, 7 μm) column and a Shimadzu RID-10A refractive index detector (Shimadzu, Kyoto, Japan). The columns were thermostated at 40 °C. pAMPTMA was eluted at a flow rate of 0.8 mL/min with 0.5 M Na_2SO_4. The number-average molecular weight (M_n) and the molecular weight distribution (M_w/M_n) were determined by calibration with near-monodisperse poly(ethylene oxide) (PEO) standards. As PEO standards were not eluted with 0.5 M Na_2SO_4 and pAMPTMA was not eluted with water, the calibration was made by eluting PEOs with water and then calculating pAMPTMA molecular weights with respect to this calibration curve using the lactose peak as elution time internal standard. The concentration of the polymeric solutions was 1 mg/mL. The injection volume was 20 μL. It was not possible to elute p(AMPTMA-*b*-NIPAAM) block copolymers with TSK-GEL α-3000 and also with TSK-GEL GM-PW (30 × 7.5 mm, 17 μm) columns using several different eluents (0.1 M $NaNO_3$:acetonitrile 80:20 (v/v), 0.2 M $NaNO_3$ and 0.5 M Na_2SO_4, water).

2.5.4. Fluorescence measurements

Steady-state fluorescent spectra were measured using a Cary Eclipse (Varian) spectrometer equipped with a thermostated cell compartment. The fluorescence emission spectra (350–550 nm) were measured using an excitation wavelength of $\lambda_{ex} = 334$ nm. The intensity ratio (I_1/I_3) of the first (I_1) over the third (I_3) vibronic band of the emission spectrum of pyrene, at 373 and 384 nm, respectively, was used to detect the formation of hydrophobic microdomains. The excitation spectra (250–370 nm) were measured using an emission wavelength of $\lambda_{em} = 374$ nm. The intensity ratio (I_{338}/I_{334}) was used to determine the critical micellar concentration (CMC). A stock solution of pyrene (5×10^{-7} M) in the aqueous solvent used for the measurement was prepared by adding 50 μL of a 5×10^{-4} M pyrene solution in acetone in a 50 mL volumetric flask, evaporating acetone by a nitrogen flow and adding the solvent. The solutions were stirred at room temperature overnight to reach the solubilization equilibrium of pyrene in the aqueous phase. The final pyrene concentration was 5×10^{-7} M, slightly below the saturation concentration of pyrene in water at 22 °C.

For the determination of the critical micellar concentration (CMC) the solutions at different polymer concentrations (1×10^{-4}–20 mg/mL) were prepared by dissolving proper amount of polymer in a given amount of 5×10^{-7} M pyrene 0.1 M NaCl aqueous solution. The solutions were heated stepwise from 25 to 60 °C. Once brought to a desired temperature within this range, the sample was

kept at that temperature for at least 10 min before measurement in order to obtain a constant value of the emission intensity. Measurements were repeated three times at each temperature.

2.5.5. Refrective index increment (dn/dc)

d*n*/d*c* was measured at 25 °C with a refractive index detector (Δ*n*-1000 RI, WGE Dr. Bures) working at 633 nm using the static method.

The d*n*/d*c* values of p(AMPTMA-*b*-NIPAAM) micelles in 0.1 NaCl were calculated by the equation [29,35]:

$$dn/dc_{A-B} = W_A(dn/dc)_A + W_B(dn/dc)_B \quad (1)$$

in which W_A and W_B are the mass fractions of pNIPAAM and pAMPTMA and $(dn/dc)_A$ and $(dn/dc)_B$ are their refractive index increments measured at 25 °C (0.1630 for pNIPAAM, 0.1705 for pAMPTMA). We assumed that the temperature dependence of d*n*/d*c* of the block copolymers is not significant [36]. The d*n*/d*c* values calculated for the block copolymers p(AMPTMA$_{30}$-*b*-NIPAAM$_{120}$), p(AMPTMA$_{60}$-*b*-NIPAAM$_{120}$) and p(AMPTMA$_{60}$-*b*-NIPAAM$_{50}$) were 0165, 0.167 and 168, respectively.

2.5.6. Dynamic light scattering (DLS)

DLS data were obtained with a Brookhaven Instruments Corp. BI-200SM goniometer equipped with a BI-9000AT digital correlator using a solid-state laser (125 mW, $\lambda = 532$ nm). If not otherwise stated, measurements of scattered light were made at a scattering angle θ of 90°. The temperature of the copolymer solution was controlled with an accuracy of 0.1 °C. All samples were first prepared by filtering about 3 mL of solution with a 0.20 μm Millipore filter into a clean scintillation vial. To determine the LCST, the temperature was raised at 0.5 °C/min and the solution was allowed to equilibrate until a stable reading of the intensity was obtained. Data were acquired for 5–20 min, and each experiment was repeated two or more times. Monomodal cumulants analysis or CONTIN analysis was used to fit the data.

2.5.7. Static light scattering (SLS)

The block copolymers were dissolved in NaCl aqueous solution at room temperature to obtain concentrations ranging from 1 to 10 mg/mL. All samples were filtered as described above. The solution was introduced in the measuring compartment at room temperature, heated at 60 °C for about 40 min and allowed to equilibrate until a stable reading of the intensity was obtained.

2.5.8. Energy filtered-transmission electron microscopy (EF-TEM)

The samples were observed in a Zeiss EM902 Transmission Electron Microscope (TEM), operating at 80 kV and equipped with an "in-column" electron energy filter. The filter was settled to collect only elastic electrons ($\Delta E = 0$), with the result to enhance image contrast and resolution due to the elimination of the inelastic electrons in the image formation (reduction of the chromatic aberration). Samples were negative stained by a 2% w/v solution of phosphotungstic acid (PTA) buffered at pH = 7.3. All the manipulations of the samples were carried out inside an oven at 60 °C. Briefly, a droplet of an aqueous solution of the copolymer (1 mg/mL), without NaCl and heated at 60 °C, was deposited onto 400 mesh copper grids covered with a very thin (about 20 nm) amorphous carbon film. The excess of liquid was removed by placing the grid onto the filter paper. Finally, the grid was dried in the oven and stained by adding a droplet of the stain solution. The excess was removed by filter paper and the sample allowed to dry.

3. Results and discussion

3.1. AMPTMA polymerization

AMPTMA was polymerized in the same conditions used by our group for other acrylamide monomers in water-DMF mixed solvents [21,37,38]. This solvent should allow the synthesis of NIPAAM and AMPTMA block copolymers in a homogeneous polymerization (Scheme 1).

In water:DMF 50:50 at 20 °C, [AMPTMA] = 1.25 M and [AMPTMA]:[ECP]:[CuCl]:[Me$_6$TREN] = 60:1:1:1 the polymerization was well controlled. The first order kinetic plot was linear up to 98% conversion indicating that the number of active species remains fairly constant and termination reactions were not significant up to very high conversion (Fig. 1). The polymerization was very fast, reaching 98% conversion in 27 min. Polymers with well-controlled molecular weight and polydispersity index (PDI) were obtained (Fig. 2). Number-average molecular weight determined by GPC increased linearly with conversion even though they are lower than the theoretical values. This is probably due to the use of relative calibration with PEO standards. Nevertheless, PDI decreased during the course of the polymerization reaching low values (1.12) at high conversion (98%).

The most discriminating test for the living character of ATRP is an efficient chain extension. AMPTMA was homopolymerized to very high conversion (>95%), and then a second batch of AMPTMA was added to this polymerizing solution. Provided that the polymer chain ends were still active, chain extension could be readily monitored by GPC. The results are reported in Fig. 3. AMPTMA was polymerized using [AMPTMA]:[ECP] = 50:1, then when the conversion was about 97% an additional amount of AMPTMA was added ([AMPTMA]:[ECP] = 200:1). The conversion of the second AMPTMA feed was 78%. The chromatograms show that the chain extension has occurred and no shoulders are present in the peak of the extended polymer. These mean that no significant amount of polymer chain ends became deactivated toward the end of the first-stage polymerization. Therefore, these ATRP conditions can be used for the synthesis of block copolymers of AMPTMA and NIPAAM using a "one-pot" approach.

3.2. Synthesis of p(AMPTMA-b-NIPAAM) block copolymers

For the synthesis of p(AMPTMA$_{60}$-*b*-NIPAAM$_{120}$), in the first stage AMPTMA was polymerized in DMF:H$_2$O 50:50 (v/v) at 20 °C using [AMPTMA]:[ECP]:[CuCl]:[Me$_6$TREN] = 60:1:1:1. When AMPTMA conversion was approximately 98%, a 4 M solution of NIPAAM

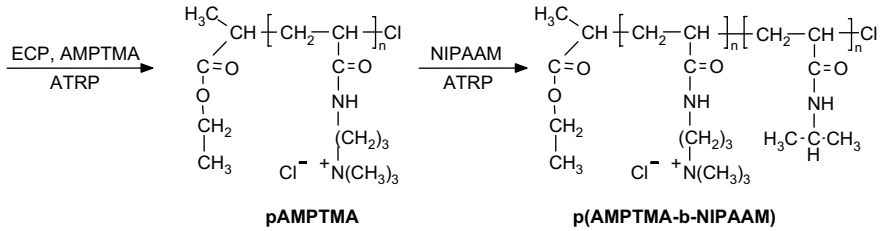

Scheme 1.

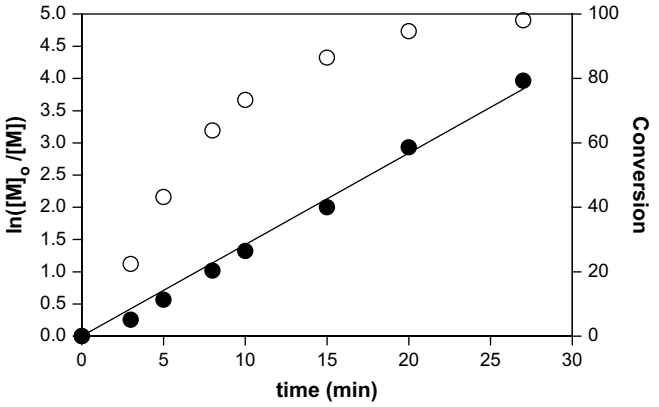

Fig. 1. First order kinetic plot (full symbols) and conversion (open symbols) for ATRP of AMPTMA in DMF:H_2O 50:50 (v/v) at 20 °C. [AMPTMA] = 1.25 M, [AMPTMA]:[ECP]:[CuCl]:[Me_6TREN] = 60:1:1:1.

([NIPAAM]:[ECP] = 200:1) in DMF:H_2O 50:50 (v/v) was added to obtain a 2 M final concentration of NIPAAM in the polymerization mixture. The first order kinetic plot was linear (Fig. 4) and the polymerization was stopped at about 60% conversion to obtain a pNIPAAM block having $X_n = 120$. In this way, three block copolymers were prepared, p(AMPTMA$_{30}$-*b*-NIPAAM$_{120}$), p(AMPTMA$_{60}$-*b*-NIPAAM$_{120}$) and p(AMPTMA$_{60}$-*b*-NIPAAM$_{50}$).

It was not possible to obtain the molecular weight distribution of the block copolymers neither with GPC nor with MALDI-TOF analysis. The copolymers were retained in the GPC columns with all the column–eluent combinations used (see Section 2). Nevertheless, by using the eluting conditions of pAMPTMA (0.5 M Na_2SO_4) with lactose internal standard we did not detect free pAMPTMA in p(AMPTMA-*b*-NIPAAM) samples, which means that all pAMPTMA initiated the polymerization of NIPAAM.

3.3. NMR spectroscopy

Fig. 5 shows the ^{1}H NMR spectrum of p(AMPTMA$_{60}$-*b*-NIPAAM$_{120}$) recorded at 20 °C. At this temperature the block copolymer is in the form of non-associated unimers and the spectrum contains the expected peaks. The relative content in pAMPTMA and pNIPAAM was calculated by the integration of the CH_3 signal (4) of pNIPAAM at about 3.8 ppm and the signals d, e and f of pAMPTMA.

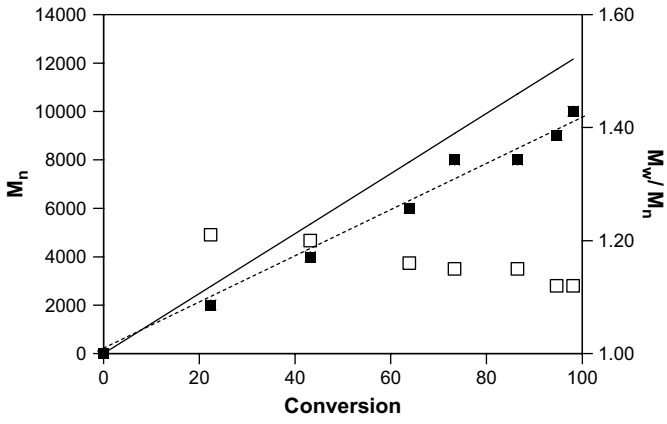

Fig. 2. Evolution of molecular weight (filled symbols) and polydispersity (open symbols) with conversion for AMPTMA in DMF:H_2O 50:50 (v/v) at 20 °C. [AMPTMA] = 1.25 M, [AMPTMA]:[ECP]:[CuCl]:[Me_6TREN] = 60:1:1:1. The straight line represents the theoretical molecular weights expected on the basis of the [AMPPTMA]/[ECP] ratio. The dashed line is the linear best fitting of the experimental data.

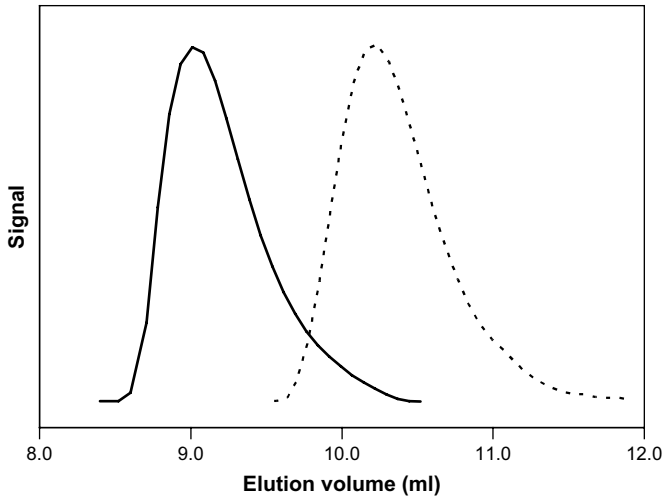

Fig. 3. GPC traces of chain-extension experiment of pAMPTMA in DMF:H_2O 50:50 (v/v) at 20 °C. [AMPTMA] = 1.25 M. (---): first block [AMPTMA]:[ECP]:[CuCl]:[Me_6TREN] = 50:1:1:1, conversion = 95%. (—): second block [AMPTMA]:[ECP]:[CuCl]:[Me_6TREN] = 200:1:1:1 conversion = 78%.

The values were in good agreement (within 10%) with the theoretical values calculated from the monomer conversion obtained by HPLC confirming the composition of the block copolymers.

^{1}H NMR was also used to have an evidence of the heat-induced association of the block copolymers in D_2O. p(AMPTMA$_{60}$-*b*-NIPAAM$_{120}$) spectra at 20 and 60 °C are reported in Fig. 5. The intensities of the peaks (3 and 4) due to the isopropyl protons of the pNIPAAM block decrease as the temperature is increased. This is consistent with a decrease of the motion of the pNIPAAM chains as a consequence of their collapse at temperature higher than LCST and incorporation in the hydrophobic core of the associated species. The pNIPAAM peaks' intensity does not completely disappeared, but decreased only about 30% probably as a consequence of a significant residual degree of mobility of pNIPAAM core due to the presence of a meaningful amount of water as already reported by other authors [8,29,39].

3.4. Fluorescence measurements

Fluorescence spectroscopy is a well-established method to detect micelle formation by using a molecular probe whose emission and

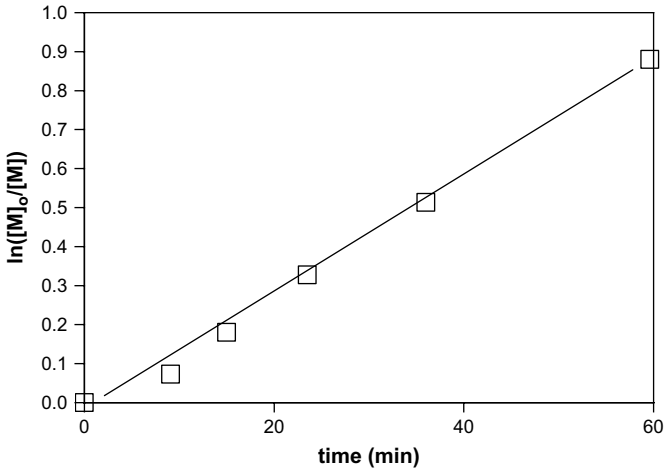

Fig. 4. First order kinetic plot for ATRP of NIPAAM in the synthesis of p(AMPTMA$_{60}$-*b*-NIPAAM$_{120}$). DMF:H_2O 50:50 (v/v), 20 °C, [NIPAAM] = 2 M, [NIPAAM]:[pAMPTMA]:[CuCl]:[Me_6TREN] = 200:1:1:1.

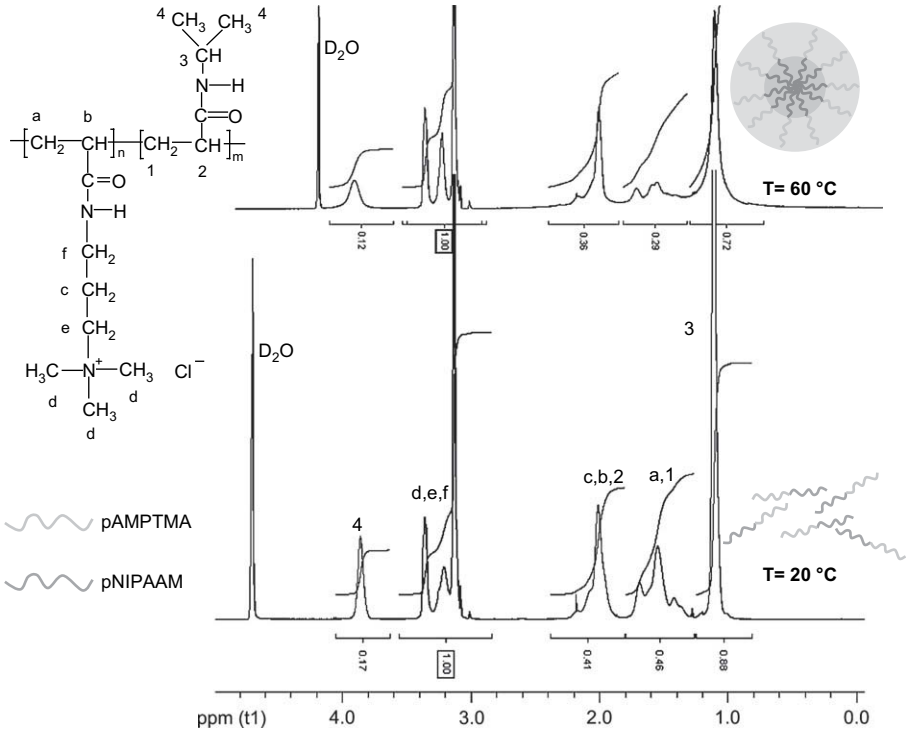

Fig. 5. 600 MHz ^{1}H NMR spectra of p(AMPTMA$_{60}$-*b*-NIPAAM$_{120}$) in D_2O at 20 and 60 °C. Polymer concentration of 10 mg/mL.

excitation spectra are sensitive to the surrounding environment, pyrene being a good example [40–42]. The I_1/I_3 ratio, used to characterize the polarity of pyrene environment, was measured in NaCl 0.1 M aqueous solutions at 60 °C by changing the polymer concentration from 10^{-4} to 20 mg/mL (Fig. 6). I_1/I_3 was about 1.80 at low concentration, meaning that no association occurs. As the concentration is raised, I_1/I_3 decreases to about 1.30, confirming micelles formation. Thus, above LCST of pNIPAAM chains, the temperature induces aggregation of the water-insoluble blocks of pNIPAAM, and the block copolymer becomes amphiphilic. It has to be noted that the plateau values after the transition are not as low as expected for a hydrophobic environment in micelles [43]. This could be due to the more polar structure of PNIPAAM or to the retention of some water in the micellar core. The critical micellar concentration (CMC) of the block copolymers was determined by measuring the excitation spectra, which show a red shift of the (0,0) band from 334 to 338 nm

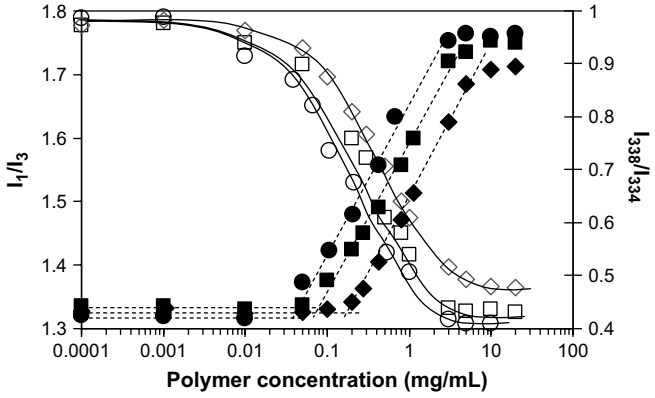

Fig. 6. I_1/I_3 (open symbols) and I_{338}/I_{334} (filled symbols) of pyrene as a function of block copolymer concentration. p(AMPTMA$_{30}$-*b*-NIPAAM$_{120}$) (○), p(AMPTMA$_{60}$-*b*-NIPAAM$_{120}$) (□), p(AMPTMA$_{60}$-*b*-NIPAAM$_{50}$) (◇). NaCl 0.1 M, $T = 60$ °C. $[Py] = 5.0 \times 10^{-7}$ M.

(characterized by change of I_{338}/I_{334} intensity ratio) upon the increase of the block copolymer concentration. Overall, these changes in the emission and excitation spectra are indicative of the partitioning of pyrene between aqueous and hydrophobic environments. The critical micellization concentration (CMC) was determined by the crossover points in the low concentration range (Fig. 6). The CMC was 0.04 mg/mL for p(AMPTMA$_{30}$-*b*-NIPAAM$_{120}$), 0.08 mg/mL for p(AMPTMA$_{60}$-*b*-NIPAAM$_{120}$) and 0.2 mg/mL for p(AMPTMA$_{60}$-*b*-NIPAAM$_{50}$), similar to the values obtained for other pNIPAAM block copolymers [21,44]. The lower CMC value was observed for p(AMPTMA$_{30}$-*b*-NIPAAM$_{120}$), confirming the influence of the pAMPTMA block length. Reasonably, the shielding of the hydrophobic pNIPAAM block above the LCST in the unimer may become more effective as the length of the ionic pAMPTMA block is increased. Second, the longer the pAMPTMA block is, the stronger is the electrostatic repulsion of pAMPTMA chains in the micelle corona. Both factors should hamper micellization, thereby increasing CMC, by, on one hand, stabilizing unimers in solutions and, on the other hand, destabilizing multimolecular micelles.

The partitioning of pyrene into the pNIPAAM core of the multimolecular associated species can be measured by the partitioning equilibrium constant K_v according to the approach proposed by Wilhelm et al. [40] According to this method, the ratio of pyrene in the micellar ($[Py]_M$) and water ($[Py]_W$) phases can be expressed as follows:

$$[Py]_M/[Py]_W = (F - F_{min})/(F_{max} - F) \quad (2)$$

where $F = I_{338}/I_{334}$, F_{min} and F_{max} are the I_{338}/I_{334} values determined at the zero copolymer concentration and at the saturating copolymer concentration, respectively. Using this model, the data can be recalculated and linearized by the following equation:

$$[Py]_M/[Py]_{H_2O} = K_v X c/1000\rho \quad (3)$$

c is the total copolymer concentration in g/L, X is the weight fraction of pNIPAAM in the copolymer, ρ is the density of the pNIPAAM

core in the micelle (which was assumed to have the same value as that of the bulk pNIPAAM, 1.070 g/mL).[45] Therefore, by plotting the $[Py]_M/[Py]_W$ ratio determined from fluorescence excitation spectra vs the copolymer concentration, the K_v value can be determined by fitting the plot above the CMC with a straight line. K_v was 3.53×10^3 for p(AMPTMA$_{30}$-*b*-NIPAAM$_{120}$), 2.74×10^3 for p(AMPTMA$_{60}$-*b*-NIPAAM$_{120}$) and 1.72×10^3 for p(AMPTMA$_{60}$-*b*-NIPAAM$_{120}$). As expected, the higher value was obtained for the copolymer with the shorter pAMPTMA block. These values are significantly lower than the values reported for other block copolymers containing polystyrene as hydrophobic segment [43–47], while are slightly lower than the values obtained for polymers containing the more polar 2-(2-methoxyethoxy)ethoxy groups involved in the core formation [48]. In our opinion this could be due to the more polar structure of pNIPAAM but mainly due to the presence of a significant amount of water in the core of the aggregates.

3.5. Dynamic light scattering (DLS)

Block copolymer solutions in NaCl 0.1 M were completely transparent at room temperature and remained transparent up to 60 °C. In a preceding paper, we observed that aqueous solutions of block copolymers of pNIPAAM and poly(sodium 2-acrylamido-2-methylpropanesulfonate) (AMPS) became markedly turbid above the LCST of pNIPAAM [21]. The increase of the scattered intensity as a function of the temperature measured at a fixed angle of 90° for a polymer concentration of 10 mg/mL in NaCl 0.1 M (Fig. 7) was used to determine the LCST of the block copolymers. LCST was determined as the intersection of the straight line passing through the inflection point of the curve and the horizontal straight line passing through the points before the transition. The LCST increases from 37.5 °C of p(AMPTMA$_{30}$-*b*-NIPAAM$_{120}$) to 44.5 °C of p(AMPTMA$_{100}$-*b*-NIPAAM$_{60}$), which means that LCST increases with increasing the AMPTMA/NIPAAM molar ratio. These values are about 4–6 °C higher than the values obtained for p(AMPS-*b*-NIPAAM) copolymers having almost the same ratio between NIPAAM and the hydrophilic block [21], which means that the pAMPTMA block has a stronger influence on the pNIPAAM transition. As shown in Fig. 8, LCST increased linearly with the NIPAAM/AMPTMA molar ratio. We observed the same behavior with p(AMPS-*b*-NIPAAM) block copolymers [21]. These results are in agreement with the data reported for not permanently charged cationic pNIPAAM block copolymers prepared by RAFT [49]. The variation of LCST should be due both to the different molecular weights of the low polydispersity pNIPAAM block [50] and to the effect of the pAMPTMA block. As reported by other authors, LCST of low polydispersity pNIPAAM in water determined by turbidity measurements ranges from about 35 to 38 °C with X_n going from 100 to 40 [50]. As the LCST of pNIPAAM depends also on salt concentration [51], the LCST values measured in 0.1 M NaCl should be increased of about 2 °C to be compared to the values in water. Therefore LCST of p(AMPTMA-*b*-NIPAAM) copolymers is 5–8 °C higher than expected for pNIPAAM with the same X_n. Thus, there is a strong effect on the pAMPTMA block that causes a significant increase of the LCST probably due to the repulsion of the polycation chains in the micelles corona.

The relaxation rates (Γ) or their distribution functions were obtained by DLS at scattering angle of 90° by a monoexponential fitting or by CONTIN analysis of the autocorrelation function.

DLS measurements were also performed at different scattering angles and Γ plotted against the square of the scattering vector q (data not reported). These plots yielded straight lines passing through the origin confirming that the observed distribution function was due to the translational diffusion of the scattering objects [52]. Therefore, the apparent hydrodynamic diameter (D_h) was determined from the Stokes–Einstein equation. The

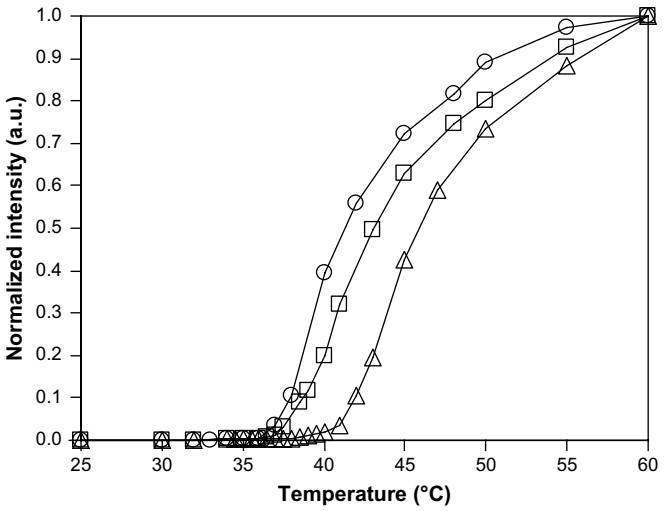

Fig. 7. Temperature dependence of the normalized scattered intensity obtained by DLS experiments at $C_p = 10$ mg/mL in 0.1 M NaCl aqueous solutions. The scattering angle was 90°. p(AMPTMA$_{30}$-*b*-NIPAAM$_{120}$) = (○), p(AMPTMA$_{60}$-*b*-NIPAAM$_{120}$) = (□), p(AMPTMA$_{60}$-*b*-NIPAAM$_{50}$) = (△).

temperature dependence of D_h at C_p 10 mg/mL in NaCl 0.1 M is reported in Fig. 9. Below the LCST the block copolymers should be molecularly dissolved (unimers) in solution. In fact, R_h values measured below the LCST were between 5 and 9 nm, confirming that the block copolymers were present in solution as unimers. It is worth mentioning that with the p(AMPS-*b*-NIPAAM) copolymers we observed the presence of loose aggregates also below the LCST [21].

Unlike the scattered intensity, there was a sharp increase of D_h above the LCST. D_h reached a maximum in one or two degrees while the scattered intensity continues to increase for several degrees. The temperature at which the onset of the increase of the hydrodynamic radius was observed corresponds to the LCST values measured by means of the scattered intensity. After the maximum, D_h slowly decreases reaching a plateau value. The presence of a maximum in the plot of D_h is probably due to the shrinking of the pNIPAAM core due to progressive dehydration [8,10,53,54]. The D_h plateau values of p(AMPTMA$_{30}$-*b*-NIPAAM$_{120}$) and p(AMPTMA$_{60}$-*b*-NIPAAM$_{120}$) were the same (47 nm) while a much lower value was obtained for p(AMPTMA$_{60}$-*b*-NIPAAM$_{50}$) (29 nm). Other authors already reported that amphiphilic ionic block copolymers with the

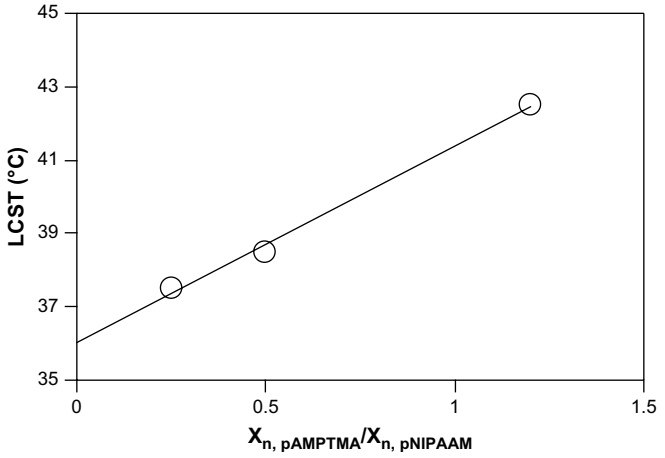

Fig. 8. LCST of the block copolymers as a function of AMPTMA/NIPAAM molar ratio. $C_p = 10$ mg/mL, 0.1 M NaCl aqueous solution.

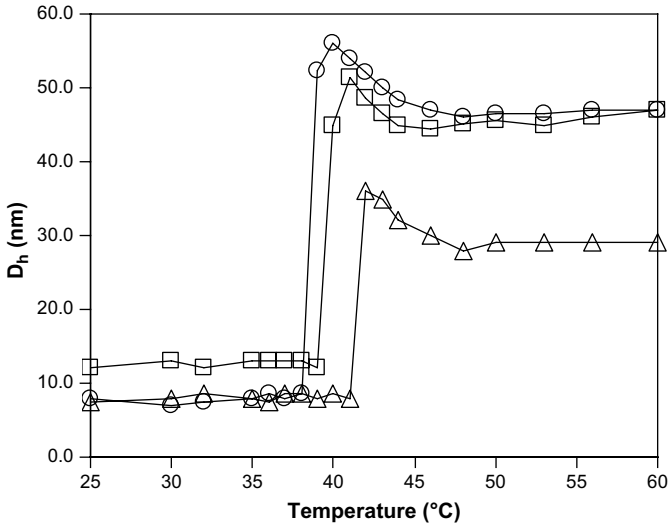

Fig. 9. Temperature dependence of the hydrodynamic diameter (D_h) obtained by DLS experiments at $C_p = 10$ mg/mL in 0.1 M NaCl aqueous solutions. The scattering angle was 90°. p(AMPTMA$_{30}$-*b*-NIPAAM$_{120}$) = (○), p(AMPTMA$_{60}$-*b*-NIPAAM$_{120}$) = (□), p(AMPTMA$_{60}$-*b*-NIPAAM$_{50}$) = (△).

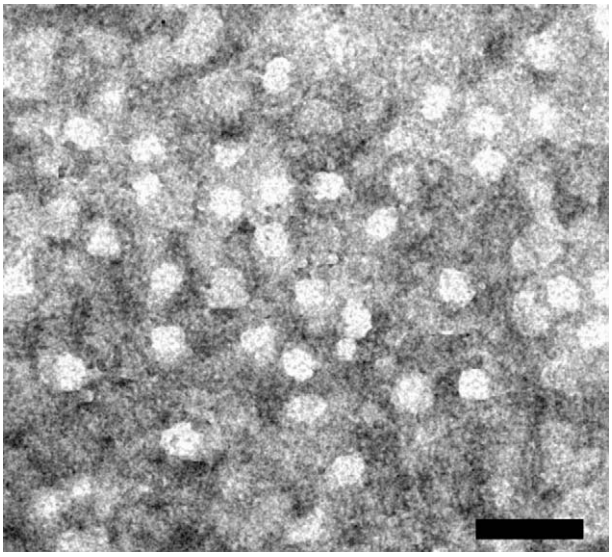

Fig. 10. TEM images of associated species obtained from p(AMPTMA$_{30}$-*b*-NIPAAM$_{120}$) in aqueous solution. Staining with 2% phosphotungstic acid. Scale bar = 100 nm.

same length of the hydrophobic block and the ionic block of different lengths had the same size [55]. We will further discuss these results later. We also found that the Γ/q^2 values are almost independent of q^2, which suggests that the associated species are spherical and not much polydisperse in size [52]. If compared with the contour length (L) of fully stretched chains calculated assuming a monomer contour length (l) of 0.25 nm, the values of D_h are compatible with the formation of core–shell micelles (Table 1).

By measuring the radius of gyration R_g by SLS we also calculated the values of the R_g/R_h ratio reported in Table 1. This parameter gives useful information about the micellar structure [56–60]. The R_g/R_h ratio for a solid sphere is well known to be 0.774 [61] while for random coils of homopolymers is about 1.50 [57]. Thus, the values obtained are much smaller than the value for homopolymers, which confirms the formation of micelles. However, compared with typical amphiphilic block copolymer crew-cut micelles (~0.775) [52,57] or the aggregates of homopolymer pNIPAAM (~0.62) formed above its LCST [62], the R_g/R_h values of the p(AMPTMA-*b*-NIPAAM) micelles are much higher, as expected due to the presence of a relatively long pAMPTMA corona. The higher value observed for p(AMPTMA$_{60}$-*b*-NIPAAM$_{50}$) with respect to the other copolymers should be due to the strong contribution of the pAMPTMA corona with respect to the smaller pNIPAAM core. This will be confirmed by the data obtained by SLS reported later.

The weight-average molar mass M_w of the micelles determined by the Zimm plot obtained by SLS was used to calculate the aggregation number N_{agg} as the ratio of M_w of the micelles to M_n of the block copolymer. It is relevant to observe that the block copolymers with the same pNIPAAM block length but different pAMPTMA blocks have almost the same R_g and R_h but have a significantly different N_{agg}. As already reported by other authors [55,63,64], N_{agg} was increased by increasing the hydrophobic block length and by decreasing the polyelectrolyte block length.

The micellar core radius R_c can be calculated assuming a spherical geometry by the equation

$$\frac{4}{3}\pi R_c^3 = \frac{N_{agg}}{N_A}\frac{M_{n,c}}{\rho} \quad (4)$$

where N_A is the Avogadro constant, and ρ is the density of the hydrophobic pNIPAAM core which is assumed to be equal to that of bulk pNIPAAM (1.070 g/mL) [45].

By subtracting the contribution of the micellar core to R_h, the thickness of the hydrophilic corona (R_s) can be estimated. With fully stretched polyelectrolyte chains, an upper limit of this thickness (L_s), corresponding to the contour length of the polyelectrolyte chains, can be calculated by knowing the degree of polymerization of the polyelectrolyte chains and assuming the length of a monomer to be equal to 0.25 nm [65]. These results are given in Table 1. p(AMPTMA$_{60}$-*b*-NIPAAM$_{50}$) micelles have pAMPTMA chains which are stretched to almost 80% of their maximum extension, as already obtained for other ionic micelles [55,63,66]. A completely different result was obtained for the other two copolymers. The R_s values are higher than L_s. We think that this could be due to the underestimation of the R_c values. In fact, R_c was calculated assuming the density of the pNIPAAM core equal to that of bulk pNIPAAM. If some water is retained in the micellar core after the transition the core will be "swelled" with respect to the bulk pNIPAAM and R_c will be higher than the calculated one. In this way, the R_s values will be overestimated.

3.6. Energy filtered-transmission electron microscopy

To obtain EF-TEM images representative of the associated copolymers, sample preparation and staining were made working at temperature above the LCST. A representative micrograph of the micelles formed by one of the block copolymer is reported in Fig. 10.

Table 1
Association properties of p(AMPTMA-*b*-NIPAAM) copolymers obtained by DLS and SLS in NaCl 0.1 M. $T = 60$ °C. DLS measurements were done at $C_p = 10$ mg/mL.

Sample	LCST (°C)	R_h (nm)	R_g (nm)	R_g/R_h	M_w (10^6)	N_{agg}	R_c (nm)	R_s (nm)	L_s (nm)	L (nm)
p(AMPTMA$_{30}$-*b*-NIPAAM$_{120}$)	37.5	23.5	21.4	0.93	3.12	158	9.2	14.3	7.5	37.5
p(AMPTMA$_{60}$-*b*-NIPAAM$_{120}$)	38.5	23.5	22.5	0.91	1.17	45	6.0	17.5	15.0	45.0
p(AMPTMA$_{60}$-*b*-NIPAAM$_{50}$)	41.5	14.5	14.7	1.01	0.45	25	3.3	11.2	15.0	27.5

The formation of small spherical particles not much polydisperse in size with an average diameter of about 30–50 nm is clearly documented, in good agreement with the results obtained by DLS.

In conclusion, we have reported the synthesis by ATRP of well-defined double hydrophilic block copolymers of pNIPAAM and pAMPTMA with different block lengths. The copolymers showed a well-defined temperature induced transition from unimers to micelles of nanometer size. The LCST and the size of the associated species were strongly affected by the relative length of the blocks. With respect to anionic block copolymers of pNIPAAM of similar composition, these block copolymers have a significantly higher LCST. The determination core and shell size demonstrated that polycation chains in the corona are markedly stretched and that a significant amount of water is retained in the pNIPAAM core after the thermo-induced transition. These kinds of block copolymers having a cationic permanently charged block are extremely interesting as they could be used in the field of gene delivery or for the synthesis of well-defined nanometer sized silica particles.

Acknowledgements

This work has been carried out with the financial support of the University "La Sapienza" (Ateneo Funds).

References

[1] Gohy JF. Adv Polym Sci 2005;190:65.
[2] Hadjichristidis N, Iatrou H, Pitsikalis M, Pispas S, Avgeropoulos A. Prog Polym Sci 2005;30:725.
[3] Riess G. Prog Polym Sci 2003;28:1107.
[4] Rodriguez-Hernandez J, Checot F, Gnanou Y, Lecommandoux S. Prog Polym Sci 2005;30:691.
[5] Heskins M, Guillet JE. J Macromol Sci Chem 1968;A2:1441.
[6] Yoshida R, Uchida K, Kaneko Y, Sakai K, Kikuchi A, Sakurai Y, et al. Nature 1995;374:240.
[7] Ge Z, Luo S, Liu S. J Polym Sci Part A Polym Chem 2006;44:1357.
[8] Skrabania K, Li W, Laschewsky A. Macromol Chem Phys 2008;209:1389.
[9] You YZ, Zhou QH, Manickam DS, Wan L, Mao GZ, Oupicky D. Macromolecules 2007;40:8617.
[10] Yusa S, Shimada Y, Mitsukami Y, Yamamoto T, Morishima Y. Macromolecules 2004;37(20):7507.
[11] Schilli CM, Zhang MF, Rizzardo E, Thang SH, Chong YK, Edwards K, et al. Macromolecules 2004;37:7861.
[12] Nuopponen M, Ojala J, Tenhu H. Polymer 2004;45:3643.
[13] Lokitz BS, Convertine AJ, Li Y, McCormick CL. Macromolecules 2006;39:8594.
[14] Convertine AJ, Lokitz BS, Vasileva Y, Myrick LJ, Scales CW, Lowe AB, et al. Macromolecules 2006;5:1724.
[15] Zhang W, Zhou X, Li H, Fang Y, Zhang G. Macromolecules 2005;38:909.
[16] Hong CY, You YZ, Pan CY. J Polym Sci Part A Polym Chem 2004;42:4873.
[17] Hales M, Barner-Kowollik C, Davis TP, Stenzel MH. Langmuir 2004;20:10809.
[18] Tang T, Castelletto V, Parras P, Hamley IW, King SM, Roy D, et al. Macromol Chem Phys 2006;207:1718.
[19] Zhang WQ, Shi LQ, Ma RJ, An YL, Xu YL, Wu K. Macromolecules 2005;38:8850.
[20] Kizhakkedathu JN, Kumar KR, Goodman D, Brooks DE. Polymer 2004;45:7471.
[21] Masci G, Diociaiuti M, Crescenzi V. J Polym Sci Part A Polym Chem 2008;46(14):4830.
[22] Xu Y, Shi L, Ma R, Zhang W, An Y, Zhu XX. Polymer 2007;48:1711.
[23] Li G, Shi L, Ma R, An Y, Huang N. Angew Chem Int Ed 2006;45:4959.
[24] Heredia KL, Bontempo D, Ly T, Byers JT, Halstenberg S, Maynard HD. J Am Chem Soc 2005;127:16955.
[25] Zhang W, Jiang X, He Z, Xiong D, Zheng P, An Y, et al. Polymer 2006;47:8203.
[26] Li G, Shi L, An Y, Zhang W, Ma R. Polymer 2006;47:4581.
[27] Bontempo D, Li RC, Ly T, Brubaker CE, Maynard HD. Chem Commun 2005;37:4702.
[28] Hasan E, Zhang M, Mueller A, Tsvetanov CB. J Macromol Sci Pure Appl Chem 2004;A41(5):467.
[29] Zhang W, Shi L, Wu K, An Y. Macromolecules 2005;38:5743.
[30] Ikeda I, Tazuke S, Suzuki Y. Makromol Chem 1984;185:869.
[31] Ravikumar T, Murata H, Koepsel RR, Russell AJ. Biomacromolecules 2006; 7:2762.
[32] Gilbert P, Moore LE. J Appl Microbiol 2005;99:703.
[33] Yuan JJ, Mykhaylyk OO, Ryan AJ, Armes SP. J Am Chem Soc 2007;129:1717.
[34] Xia J, Gainor SG, Matyjaszewski K. Macromolecules 1998;31:5958.
[35] Virtanen J, Holappa S, Lemmetyinen H, Tenhu H. Macromolecules 2002;35:4763.
[36] Qiu X, Wu C. Macromolecules 1997;30:7921.
[37] Masci G, Giacomelli L, Crescenzi V. J Polym Sci Part A Polym Chem 2005;43(19):4446.
[38] Masci G, Giacomelli L, Crescenzi V. Macromol Rapid Commun 2004;25(4):559.
[39] Virtanen T, Tenhu H. Macromolecules 2000;33:5970.
[40] Wilhelm M, Zhao C-L, Wang Y, Xu R, Winnik MA, Mura J-L, et al. Macromolecules 1991;24:1033.
[41] Kalyanasundaram K, Thomas JK. J Am Chem Soc 1977;99:2039.
[42] Lianos P, Viriot M-L, Zana R. J Phys Chem 1984;88:1098.
[43] Lysenko EA, Bronich TK, Slonkina EV, Eisenberg A, Kabanov VA, Kabanov AV. Macromolecules 2002;35:6351.
[44] Topp MDC, Dijkstra PJ, Talsma H, Feijen J. Macromolecules 1997;30:8518.
[45] Shields DJ, Coover HW. J Polym Sci 1959;39:532.
[46] Astafieva I, Zhong X, Eisenberg A. Macromolecules 1993;26:7339.
[47] Cao T, Munk P, Ramireddy C, Tuzar Z, Webber SE. Macromolecules 1991; 24:6300.
[48] Chang Y, Lee S, Kim KT, Kim C, Reeves SD, Allcock HR. Macromolecules 2001;34(2):269.
[49] Li Y, Lokitz BS, McCormick CL. Angew Chem Int Ed 2006;45:5792.
[50] Xia Y, Yin X, Burke NAD, Sto1ver HDH. Macromolecules 2005;38:5937.
[51] Bokias G, Staikos G, Iliopoulos I. Polymer 2000;41:7399.
[52] Xu R, Winnik MA, Hallett FR, Riess G, Croucher MD. Macromolecules 1991;24:87.
[53] Verbrugghe S, Laukkanen A, Aseyev V, Tenhu H, Winnik FM, Du Prez FE. Polymer 2003;44:6807.
[54] Aseyev V, Hietala S, Laukkanen A, Nuopponen M, Confortini O, Du Prez FE, et al. Polymer 2005;46:7118.
[55] Burguière C, Chassenieux C, Charleux B. Polymer 2003;44(3):509.
[56] Burchard W. Adv Polym Sci 1983;48:1.
[57] Tu Y, Wan X, Zhang D, Zhou Q, Wu C. J Am Chem Soc 2000;122:10201.
[58] Wu C, Zuo J, Chu B. Macromolecules 1989;22:633.
[59] Antonietti M, Heinz S, Schimidt M. Macromolecules 1990;23:3796.
[60] Antonietti M, Wremser W, Schimidt M, Rosenauer C. Macromolecules 1994;27:3276.
[61] Mallamace F, Micali N. In: Brown W, editor. Low angle light scattering and its applications in light scattering: principles and development. Oxford: Clarendon Press; 1996. p. 381.
[62] Wu C, Zhou S. Macromolecules 1995;28:8381.
[63] Khougaz K, Astafieva I, Eisenberg A. Macromolecules 1995;28:7135.
[64] Forster S, Zisenis M, Wenz E, Antonietti MJ. Chem Phys 1996;104:9956.
[65] Zhang L, Barlow RJ, Einsenberg A. Macromolecules 1995;28:6055.
[66] Forster S, Hermsdorf N, Bottcher C, Lindner P. Macromolecules 2002;35:4096.